Available online at www.sciencedirect.com

ScienceDirect

Energy Procedia 63 (2014) 5762 – 5772

Energy Procedia

GHGT-12

Effect of heat treatment of injection pipe steels on the reliability of a saline aquifer water CCS-site in the Northern German Basin

Anja Pfennig[a]*, Helmut Wolthusen[a], Marcus Wolf[a] and Axel Kranzmann[b]

[a] *HTW University of Applied Sciences Berlin, Wilhelminenhofstraße 75 A, Gebäude C, 12459 Berlin, Germany*
[b] *BAM Federal Institute of Materials Research and Testing, Unter den Eichen 87, 12205 Berlin, Germany*

Abstract

Samples of differently heat treated high alloyed stainless injection-pipe steels AISI 420 X46Cr13, AISI 420J X20Cr13 as well as X5CrNiCuNb16-4 AISI 630 were kept at T=60 °C and ambient pressure as well as p=100 bar for 700 h - 8000 h in a CO_2-saturated synthetic aquifer environment similar to possible geological on-shore CCS-sites in the northern German Basin. Corrosion rates and scale growth are lowest after long term exposure for steels hardened and tempered at 600 to 670 °C and pits - indicating local corrosion- decrease in diameter but increase in number as a function of carbon content of the steel. Martensitic microstructure is preferred with respect to this particular CCS-site.

Peer-review under responsibility of the Organizing Committee of GHGT-12

Keywords: steel; supercritical CO_2; pipeline; corrosion; CCS; CO_2-storage

1. Introduction

When compressing emission gasses from combustion processes and injecting CO_2 into deep geological saline aquifer reservoirs (CCS Carbon Capture and Storage) [1], as found in the Northern German Basin, the CO_2 is dissolved to build a corrosive environment which may easily cause failure of pipe steels [2,3]. As a result of the anodic iron dissolution of the pipe steel a siderite corrosion layer ($FeCO_3$) grows on the alloy surface [4-6]. Internal

* Corresponding author. Tel.: 49 30 5019 4231; fax: +49 30 8104 3917.
E-mail address: anja.pfennig@htw-berlin.de

Peer-review under responsibility of the Organizing Committee of GHGT-12
doi:10.1016/j.egypro.2014.11.609

corrosion will depend largely upon the source of the injected gas, its composition and the presence of water and dissolved salts. Here corrosion of the injection pipe in CO_2-rich aquifer water may be a possibility when at injection intervals, the aquifer water may flow back into the injection pipe and then form phase boundaries [5,7].

The influence of heat treatment, that is: temperature and time of austenitizing, cooling rate as well as temperature and time of annealing, has been shown by various authors: Retained austenite as a microstructural component resulting from the heat treatments applied has a beneficial effect on the pitting corrosion resistance of 13%-chromium steels (13CrNiMo) [8]. A higher Ni and Cr content in the heat treated steels improve the corrosion resistance [8-11]. In general, raising the annealing temperature lowers the pitting potential of lean duplex stainless steels [10,12-13]. The increased corrosion resistance of martensitic stainless steels with 13% Cr at higher austenitizing temperature (980-1050 °C) is related to the dissolution of carbides [14-16]. The precipitation of Cr-rich $M_{23}C_6$ and M_7C_3 carbides reduced the resistance of passive film and pitting corrosion [13] and has high impact on mechanical properties due to secondary hardening [14]. The influence of heat treatment on microstructure and mechanical properties is well known [13,16,17]. However for C-Mn (carbon) steels offering excellent mechanical strength the martensitic microstructure has the highest corrosion rate in a H_2S-containing NaCl solution up to two orders of magnitude higher than ferritic or ferritic-bainitic microstructures due to the fact that martensitic grain boundaries are more reactive [17]. Many authors demonstrate the dependence also on environmental factors, e.g. the composition of surrounding media and alloy, temperature, CO_2 partial pressure, flow conditions, contaminations and formation of protective scales [4,18,19]; in this study the influence of heat treatment of the steels prior to exposure, hydrostatic pressure within the storage site and alloying elements of the steels is analyzed for a critical temperature region well known for severe corrosion processes [3,5,7,20-25] .

2. Material and Methods

Exposure tests were carried out using samples made of thermally treated specimen of AISI 4140 (1%Cr) and AISI 420C (X46Cr13, 0.46%C, 13%Cr)), AISI 420J (X20Cr13, 0.20%C, 13%Cr) and AISI 630 (X5CrNiCuNb16-4) with 8 mm thickness and 20 mm width and 50 mm length. A hole of 3.9 mm diameter was used for sample positioning. Heat treatment prior to exposure was done following routine protocols according to the 3 steel qualities (Table 1).

Table 1: Heat treatment of steels prior to exposure to CO_2-saturated aquifer at 100 bar.

material	heat treatment	temperature °C / °C	dwell time min	cooling medium
X20Cr13 1.4021	normalizing	785	30	air
	hardening	1000	30	oil
	hardening + tempering 1, 600 °C	1000 / 600	30	oil
	hardening + tempering 2, 670 °C	1000 / 670	30	oil
	hardening + tempering 3, 755 °C	1000 / 755	30	oil
X46Cr13 1.4034 AISI 420 C	normalizing	785	30	air
	hardening	1000	30	oil
	hardening + tempering 1, 600 °C	1000 / 600	30	oil
	hardening + tempering 2, 670 °C	1000 / 670	30	oil
	hardening + tempering 3, 700 °C	1000 / 700	30	oil
	normalizing	785	30	air
X5CrNiCuNb16-4 1.4542 AISI 630	normalizing	850	30	oil
	hardening	1040	30	oil
	hardening + tempering 1, 600 °C	1040 / 550	30	oil
	hardening + tempering 2, 670 °C	1040 / 650	30	oil
	hardening + tempering 3, 700 °C	1040 / 755	30	oil

The surfaces were activated by grinding with SiC-Paper down to 120 µm under water. Samples of each base metal were positioned within the vapour phase (1 bar), the supercritical phase (100 bar) and within the liquid phase. The brine (as known to be similar to the Stuttgart Aquifer [6]: Ca^{2+}: 1760 mg/L, K^{2+}: 430 mg/L, Mg^{2+}: 1270 mg/L, Na^{2+}: 90,100 mg/L, Cl^{-}: 143,300 mg/L, SO_4^{2-}: 3600 mg/L, HCO_3^{-}: 40 mg/L) was synthesized in a strictly orderly way to avoid precipitation of salts and carbonates. The exposure of the samples between 700 h to 8000 h was disposed in a chamber kiln at 60 °C at 100 bar in an autoclave system and for reference at ambient pressure as well (figure 1). Flow control (3 NL/h) at ambient pressure was done by a capillary meter GDX600_man by QCAL Messtechnik GmbH, München.

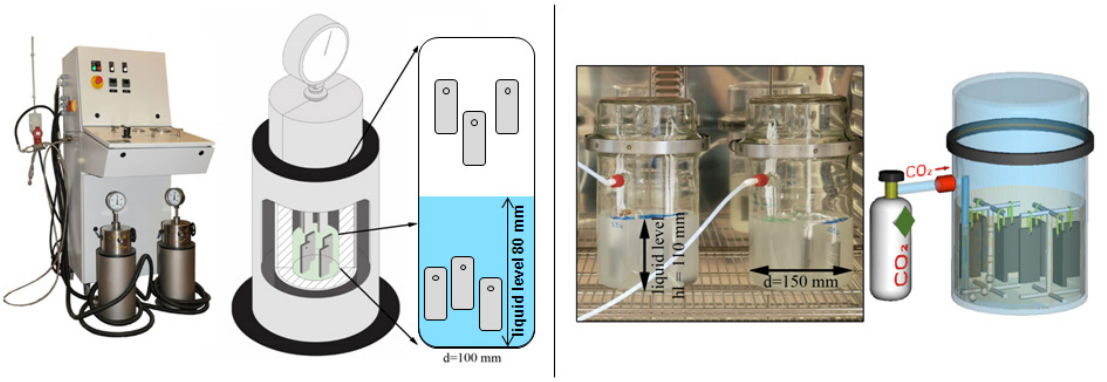

Fig. 1. Experimental set-up of laboratory corrosion experiment: left: autoclaves 100 bar/60 °C, right: ambient pressure/60 °C [26].

X-ray diffraction was carried out in a URD-6 (Seifert-FPM) with CoKα-radiation with an automatic slit adjustment, step 0.03 and count 5 sec and AUTOQUAN ® by Seifert FPM was used for phase analysis. For gravimetric measurement descaling of the samples (60°C/700 h, 2000 h, 4000 h, 8000 h) was performed by exposure to 37% HCl for 24 hours and mass gain was analyzed according to DIN 50 905 part 1-4. To characterise the pitting corrosion, 3-D-images were realized by the double optical system Microprof TTV by FRT. Non-descaled parts of the samples were embedded in a cold resin (Epoxicure, Buehler), cut and polished first with SiC-Paper from 180 µm to 1200 µm under water and then finished with diamond paste 6 µm, 3 µm and 1 µm. The measurement of the layer thicknesses and residual pipe wall thicknesses as well as microstructure analysis were performed via light and electron microscopy techniques using the semi-automatic analyzing program Analysis Docu ax-4 by Aquinto. A set of 100 linescans was measured taking 10 to 20 micrographs per parameter.

3. Results and Discussion

During the normal storage procedure the CO_2 is supposedly injected in its supercritical phase. In the case of intermissions of the injection the water level may rise into the injection pipe which may lead to the precipitation of corrosion products and formation of pits as stated. Experiments at ambient pressure with excess oxygen in the open system can overestimates the pit corrosion predicted resulting from higher corrosion rates and greater pit penetration depths at ambient pressure than at 100 bar. Specimens exposed to the brine form a carbonate layer as result of the low siderite $FeCO_3$-solubility in CO_2-containing water forming carbonic acid which results in rather low pH (figure 2). These non-uniform corrosion layer are differing in thickness but formed all over the surface. The following results were obtained for samples kept in the liquid CO_2-saturated aquifer phase.

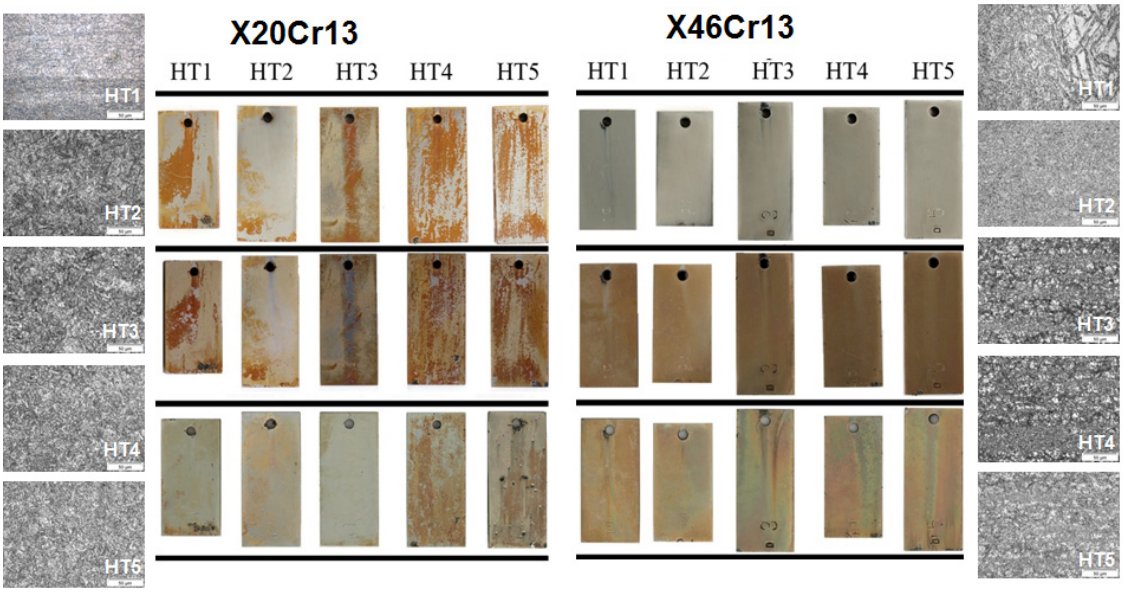

Fig. 2. Sample surfaces and microstructures of X20Cr13 and X46Cr13 after 4000 hours of at 60 °C and 100 bar to water-saturated supercritical CO_2 or liquid CO_2-saturated aquifer phase.

The multi-layered carbonate/oxide structure is described in detail by Pfennig et al. [24]. It reveals siderite $FeCO_3$, goethite a-FeOOH at 100 bar and additionally mackinawite FeS and akaganeite $Fe_8O_8(OH)_8Cl_{1.34}$ as well as spinel-phases of various compositions at ambient pressure. Also carbides, Fe_3C, were identified within the corrosion layer. Pits are covered with the same precipitates of the corrosion products formed on the surface elsewhere [23,24].

3.1. Kinetics of surface corrosion

After 8000 h of exposure at 60 °C/100 bar most steels show a decreasing corrosion rate no regard of heat treatment prior to exposure (figure 3). Figure 4 depicts the corrosion rates of the 3 steel qualities as a function of exposure time, heat treatment and pressure.

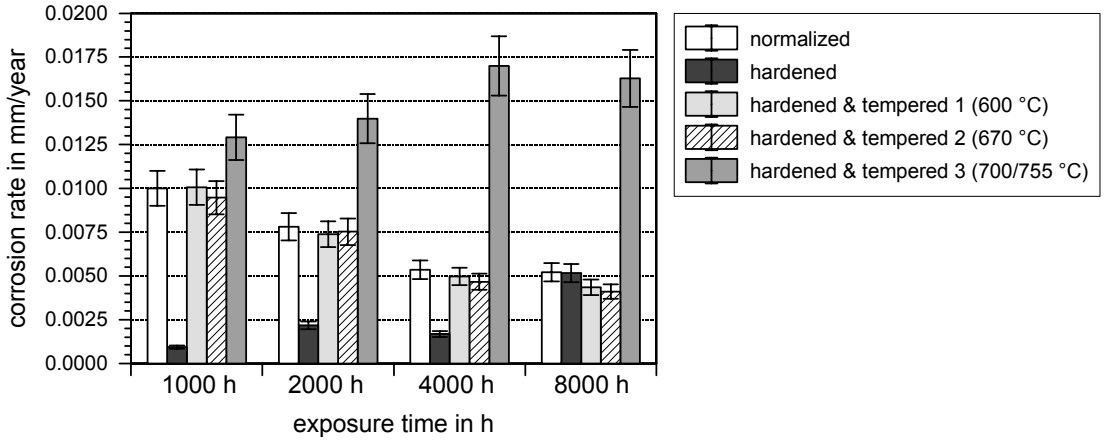

Fig. 3. Comparison of corrosion rate as a function of time of the alloys X46Cr13 and X20Cr13 (60 °C / 100 bar / CO_2 saturated brine) at 100 bar. The alloys were analyzed regarding heat treatment with no respect to alloy composition or atmosphere).

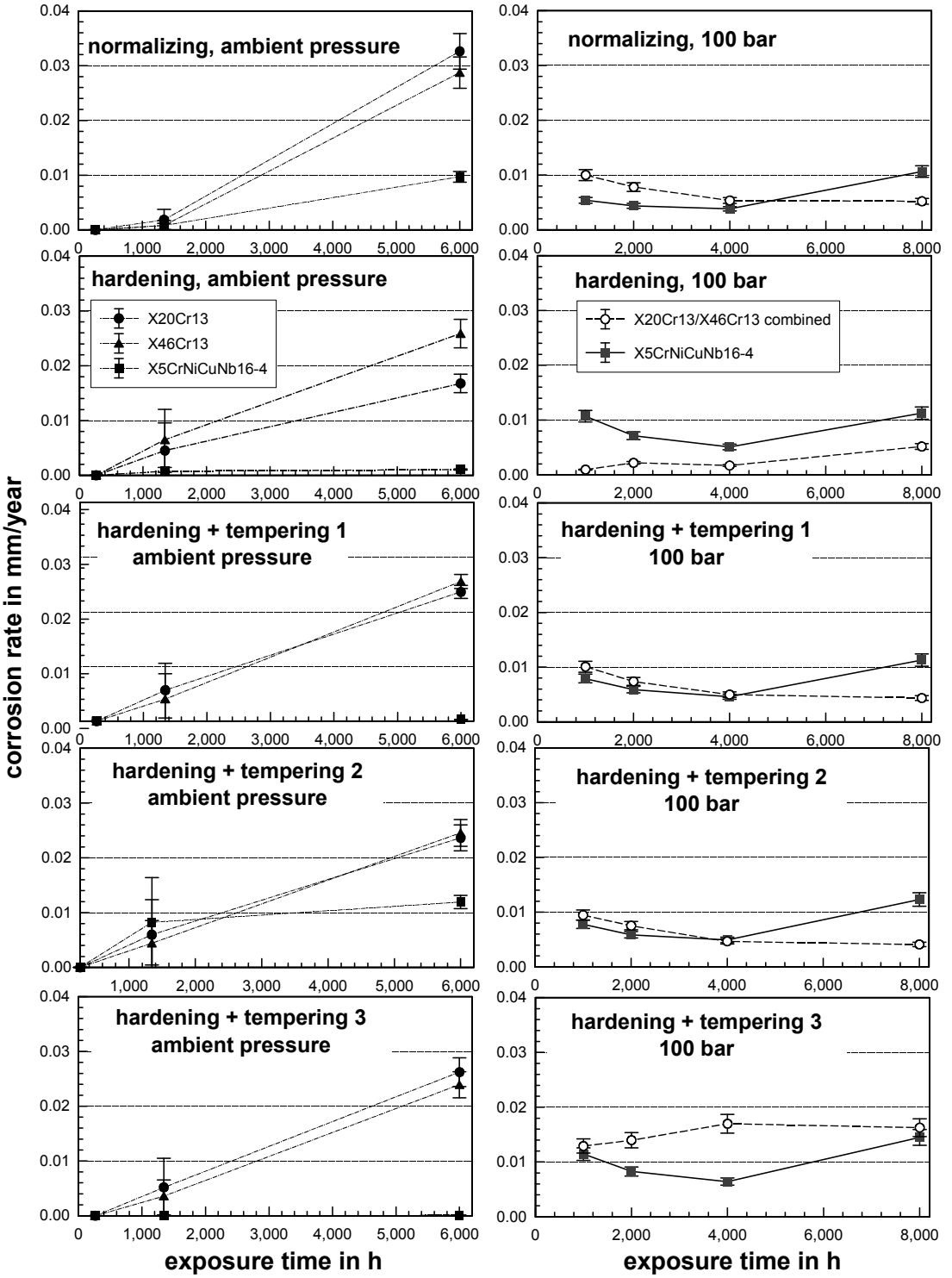

Fig. 4. Corrosion rate after 6000 and 8000 hours of exposure to CO_2-saturated aquifer water at 60 °C and ambient pressure, left and 100 bar, right of X20Cr13, X46Cr13 (combined at 100 bar) and X5CrNiCuNb16-4 heat treated prior to exposure.

The corrosion rate generally does not exceed 0.02 mm/year for differently heat treated X20Cr13 and X46Cr13 as well as X5CrNiCuNb16-4 and therefore is in good agreement with DIN 6601 allowing for 0.1 mm/year for pressure vessels. The increasing rather high corrosion rate for samples hardened and tempered at 700°C/755 °C may be due to the carbide precipitation depleting the metal matrix that surrounds the carbide of chromium and prohibits the passivation of the surface. This as a consequence leads to the degradation of the base material after long exposure to the CO_2-saturated saline aquifer environment.

Under supercritical CO_2 and saline water conditions a martensitic microstructure of hardened and tempered steel at low temperatures (600-670 °C) offers best corrosion resistance regarding surface corrosion (figure 3). Between 4000 h and 8000 h of exposure the corrosion rates do not change indicating a sufficient thickness of the carbonate layer where mutual diffusion of ionic species into the base materials (CO_3^{2-} —and O^{2-} —species) and towards the outer surface (Fe-ions) is reduced.

With corrosion rates obtained via mass gain method about 0.002 mm/year at ambient pressure X5CrNiCuNb16-4 shows the lowest loss of base material for samples that were hardened or hardened and tempered (figure 4 left). Normalized samples corrode around 0.01 mm/year determined after 6000 hours of exposure.

At 100 bar corrosion rates are similar to those obtained at ambient pressure after up to 2000 h, but after 8000 h of exposure the corrosion rates obtained under pressure are significantly lower. Here the pressure influences the corrosion rate, possibly due to closing of capillary systems and preventing fast diffusion processes after long exposure and sufficient thickness of corrosion layer. Still, hardening and tempering 2 at 670 °C give best results with lowest corrosion rates in water saturated supercritical CO_2. As a function of time there is no significant influence of exposure time after the initial corrosion reactions have taken place after ca. 1000 h. The slightly lower rates after 4000 h of exposure are most likely due to an increasing corrosion layer and therefore reduced diffusion rates of ionic species out of the steel to condense at the surface. This increase/decrease is much more present when steels are exposed to the CO_2-saturated brine with corrosion rates around 0.004 to 0.014 mm/year (figure 4, right). Additionally the corrosion rate increase further with exposure time, indicating a break-down of the passivating nature of the corrosion layer, possibly due to local lateral detachment of large areas of the corrosion layer. Normalized samples perform best under water. Still hardening+tempering X5CrNiCuNb16-4 would provide suitable corrosion resistance in a CCS-site borehole in saline aquifer environment.

3.2. Kinetics of local corrosion

Number of pits:

At ambient pressure the heat treatment has little influence on the number of pits per unit area, because there is little to no lowest amount of counted pits for one distinct heat treatment (figure 5). The least number of pits is found on X46Cr13. Comparing steels with the same chromium content of 13% the higher carbon content in, X46Cr13 (0.46% C), results only in a slightly lower number of pits compared to X20Cr13 (0.20%). Therefore the number of pits is combined in figure 5 for these 2 steels. For X20Cr13 and X46Cr13 hardening and tempering between 600°C and 670°C (1 and 2) show the lowest amount of pits after 6000 h while X5CrNiCuNb16-4 has a rather high number of pits per m^2.

Due to the lack of significant difference in number of pits comparing X20Cr13 and X46Cr 13 the number of pits are combined in figure 5 [26]. Also under high pressure there is no preferable heat treatment although hardening and tempering (1 and 2) give slightly better results. The low number of pits for hardened steels after 8000 h of exposure has to be discussed. Possibly the carbide distribution within the distinct microstructure is responsible for a low number of pits, given less carbides which are susceptible towards fast degradation under CO_2 environment.

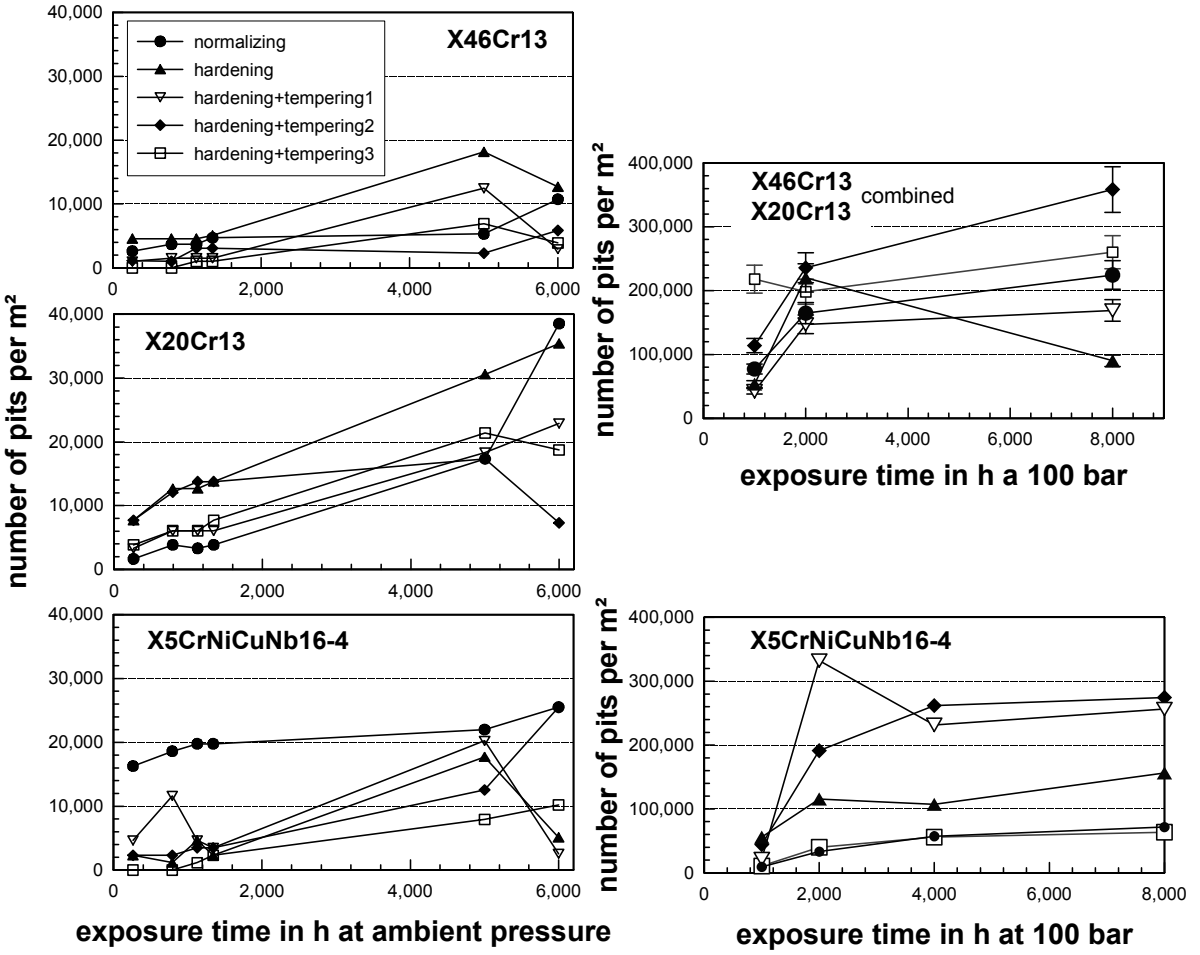

Fig. 5. Number of pits after 6000 hours and 8000 hours of exposure to CO_2-saturated aquifer water at 60 °C and ambient pressure, left and 100 bar, right of X20Cr13, X46Cr13 (combined at 100 bar) and X5CrNiCuNb16-4 heat treated prior to exposure. The graph up right was taken from Pfennig et al. [26].

At 100 bar the surface of 1.4542 exhibits surface corrosion phenomena as well as pitting corrosion. Independent of heat treatment, 1.4542 developed pitting corrosion in both phases, CO_2-saturated brine and water-saturated supercritical CO_2. The number of pits after 8000 h is 50000 -260000 per m^2 in the liquid phase (figure 5, right) and from 250000 to more than 1000000 per m^2 in the supercritical phase (not shown in figure 5). The lower amount of pits on different samples after 6000 h of exposure is due to surface corrosion phenomena: that is that pits consolidate to shallow pit corrosion and are any longer counted as single pits. These surface corrosion products prevent the access of corrosive media to the bulk material.

The most stunning finding when comparing number of pits at ambient pressure and 100 bar is that the number of pits counted after exposure at 100 bar exceeds the number of pits counted after exposure at ambient pressure by a factor of 10! This may be due to two reasons: first: the corrosion scale thickness at ambient pressure is much higher after the same exposure time and therefore pits are a lot harder to detect and process in the following microscopic

study once they lie underneath a continuous scale. Second: Kinetics at 100 bar are faster, pressing CO2 and water onto the metal`s surface resulting in a lower pH and faster degradation of the steel. This may still offer a suitable explanation although surface corrosion rates at 100 bar are generally lower than at ambient pressure. It shows definitely that local corrosion is not predictable under CCS conditions such as 100 bar, 60 °C and Stuttgart Aquifer water.

Steels will be unsuitable for its use in pressure vessel applications if the corrosion rate exceeds 0,1 mm/ year. Maximum corrosion rate in the liquid phase is approximately 0.014 mm/year, after 8000h. 1.4542 exhibited a maximum corrosion rate of approximately 0.003 mm/year in the supercritical phase. Furthermore, pitting corrosion is not allowed on specimens' surface to fulfill the regulations of DIN 6601. There is a notable risk of having a notch effect in the surface due to pitting then causing fractures and the inevitable failure of the component.

Pit intrusion depth:

Pit intrusion depths were measured for steel coupons exposed to aquifer water at 60 °C and ambient pressure. Pits were obtained metallographically and via optical volume measurement and are found on all 3 steel qualities with maximum pit intrusion depths around 300 µm for hardened X20Cr13 with martensitic microstructure after 6000 h of exposure at ambient pressure. Figure 6 reveals typical surfaces with localized corrosive attack measured via optical profilometer. Pit depths measured on X46Cr13 do not penetrate as deep as pits measured on the other steel samples (figure 7). Still, the heat treatment does not influence the maximum penetration depth significantly except for hardened samples and X5CrNiCuNb16-4 hardened+tempered at 600 °C. For the 13Cr steels (X20Cr13 and X46Cr13) normalizing and hardening+tempering at 600 °C show smaller intrusion (8-25 µm) than the other heat treatments, while hardening+tempering between 670 °C and 755 °C seem to be best for X5CrNiCuNb16-4 (10 µm).

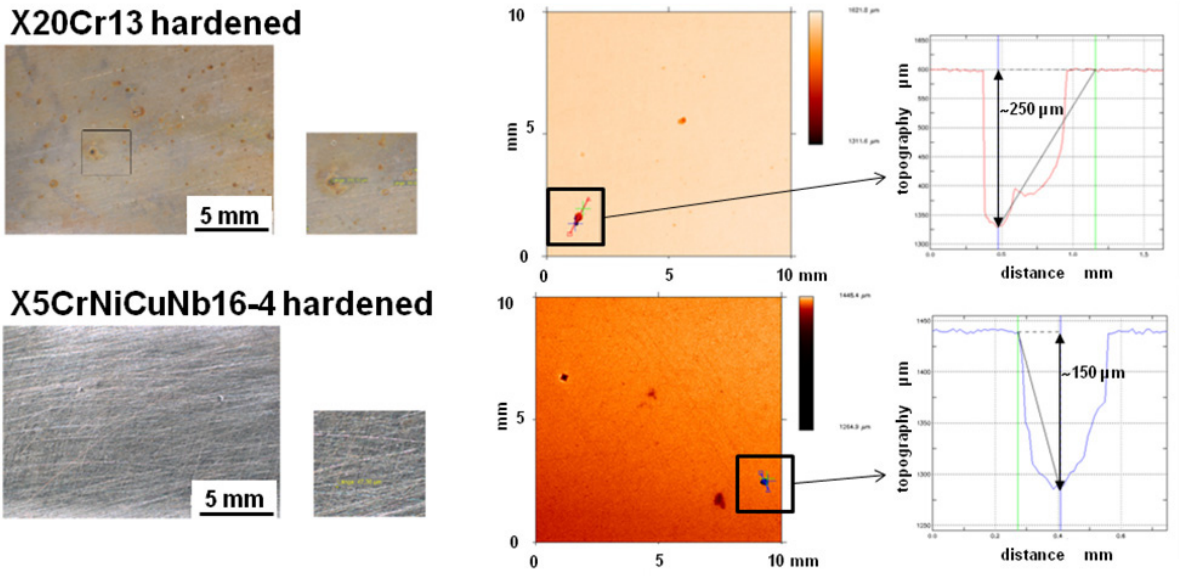

Fig. 6. Typical surfaces and surface profiles with severe pit corrosion attack after 6000 hours of exposure at 60 °C and ambient pressure of X20Cr13 and X5CrNiCuNb16-4 hardened prior to exposure.

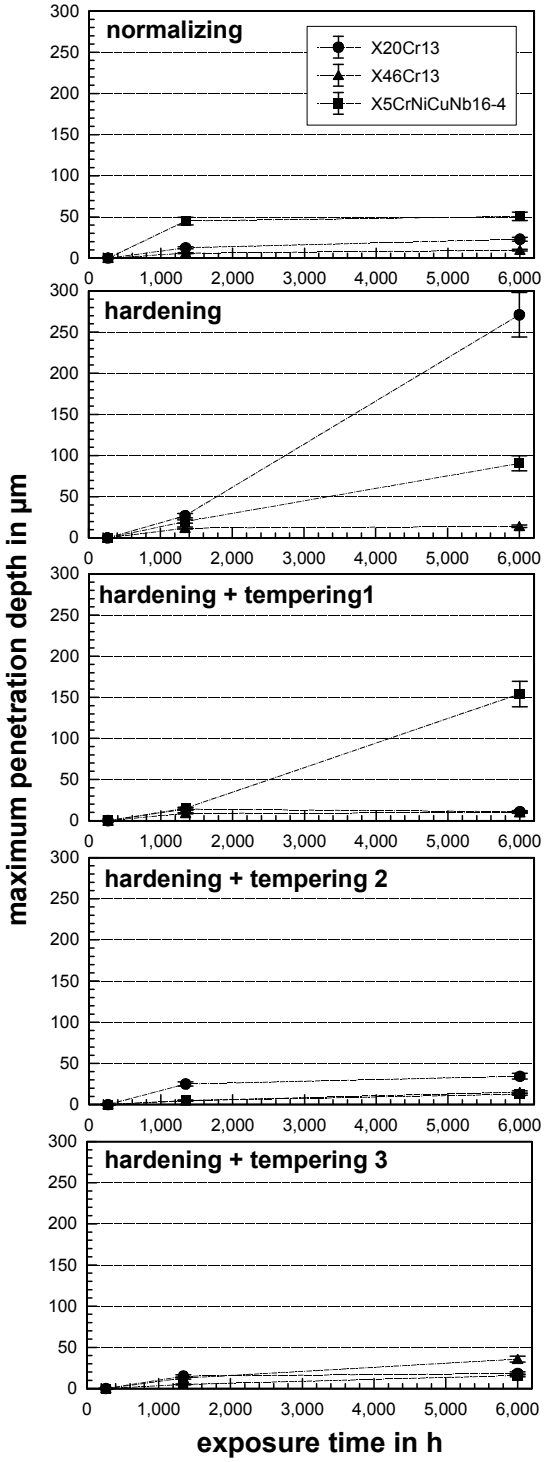

Fig. 7. Maximum penetration depth after 8000 hours of exposure to CO_2-saturated aquifer brine water at 60 °C and ambient pressure and 100 bar (X20Cr13, X46Cr13 and X5CrNiCuNb16-4).

Pit growth is a statistical phenomenon and cannot be calculated as easily as surface corrosion rates, because of its little predictability. Therefore it is not possible to give reliable corrosion rates and lifetime predictions regarding pit corrosion in CCS technology. Penetration depth of ca. 600 µm after 8 months of exposure will give pit growth rates over 0.1 mm/year [26]. Independent of the exposure time and pressure the smallest number of pits is found on steels with martensitic microstructure. Regarding steels with similar Cr-content the higher C-content in 1.4034 results in fewer pits and lower maximum intrusion depth compared to 1.4021. Despite corrosion resiting alloying elements in X5CrNiCuNb16-4 the steel is exhibits local corrosion giving more pits per unit area with rather large pit penetration depths at ambient pressure and significantly higher number of pits at 100 bar.

4. Conclusion

Differently heat treated steels used as injection pipe with 13% Chromium and 0.46% Carbon (X46Cr13, 1.4034) or 0.2% Carbon (X20Cr13, 1.4021) and 0.05% Carbon (X5CrNiCuNb16-4, 1.4542) were exposed up to 8000 h (approximately 1 year) to supercritical CO_2 and saline aquifer water at ambient pressure as well as 100 bar and 60 °C in laboratory experiments. At 100 bar and 60 °C hardening and tempering at low temperatures (600 to 670 °C) for X20Cr13 and X46Cr13 result in lowest corrosion rates. For X5CrNiCuNb16-4 hardening and tempering at 670 °C seems to give best corrosion resistance. At ambient pressure the least corrosive attack is achieved by a continuous martensitic microstructure. According to DIN 6601 both steels would be unsuitable for pressure vessel application, when being surrounded by the CO_2-saturated brine. Steels fail the conservative pressure vessel requirements no regard of heat treatment, because although the corrosion rates are all below the maximum of 0.1 mm/year, the maximum pit depth exceeds 0.2 mm. Despite low surface corrosion rates pit growth rates only allows the steel to be suitable for injection pipes in CCS environments if monitored closely [26].

Most important findings are:

a. Long term exposure tests in CCS-environment (60 °C and 100 bar) reveal that hardening and tempering at 600 °C to 670 °C has the best corrosion resistance against uniform and pitting corrosion at injection conditions. The same results are obtained at ambient pressure as well.
b. Non-uniform corrosion forms carbonate corrosion products on the surface such as siderite and goethite.
c. The higher the carbon content of the steels is usually known for reduced corrosion resistance (X20Cr13<C46Cr13). But here X46Cr13 shows slightly better corrosion resistance and lower number of pits than X20Cr13 at ambient pressure. At 100 bar there is no significant difference.
d. X5CrNiCuNb16-4 shows lower surface corrosion rates, but taken into account the local corrosion behaviour it is surprisingly not significantly performing better in CCS environment compared to the much less costly steels X20Cr13 and X46Cr13. Its usability in engineering a CCS site has to be discussed and further corrosion tests are strongly recommended.

Acknowledgement

This work was supported by the FNK (Fachkonferenz für wissenschaftlichliche Nachwuchskräfte) of the Applied University of Berlin, HTW and by IMPACT (EU-Project EFRE 20072013 2/21).

References

[1] Thomas, D.C., Carbon Dioxide Capture for Storage in Deep Geologic Formations – Results from CO_2 Capture Project, Volume 1: Capture and Separation of Carbon Dioxide form Combustion Sources, CO_2 Capture Project, Elsevier Ltd UK 2005, ISBN 0080445748.

[2] Nešić, S., Key issues related to modelling of internal corrosion of oil and gas pipelines – A review, Corrosion Science 49 (2007) 4308–4338.

[3] Carvalho, D.S., Joia, C.J.B., Mattos, O.R., Corrosion rate of iron and iron-chromium alloys in CO_2-medium, Corrosion Science 47 (2005) 2974-2986.

[4] Cui, Z.D., Wu, S.L., Zhu, S.L., Yang, X.J., Study on corrosion properties of pipelines in simulated produced water saturated with supercritical CO_2, Applied Surface Science 252 (2006) 2368-2374.

[5] Pfennig, A., Kranzmann, A., Reliability of pipe steels with different amounts of C and Cr during onshore carbon dioxid injection, International Journal of Greenhouse Gas Control 5 (2011) 757–769.

[6] Förster, A., Norden, B., Zinck-Jørgensen, K., Frykman, P., Kulenkampff, J., Spangenberg, E., Erzinger, J., Zimmer, M., Kopp, J., Borm, G., Juhlin, C., Cosma, C., Hurter, S., 2006, Baseline characterization of the CO2SINK geological storage site at Ketzin, Germany: Environmental Geosciences, V. 13, No. 3 (September 2006), pp. 145-161.

[7] Wu, S.L., Cui, Z.D., Zhao, G.X., Yan, M.L., Zhu, S.L., Yang, X.J., EIS study of the surface film on the surface of carbon steel form supercritical carbon dioxide corrosion", Applied Surface Science 228 (2004) 17-25.

[8] Bilmes, P.D., Llorente, C.L., Méndez, C.M., Gervasi, C.A., Microstructure, heat treatment and pitting corrosion of 13CrNiMo plate and weld metals, Corrosion Science 51 (2009) 876-882.

[9] Bülbül, Ş., Sun, Y., Corrosion behaviours of high Cr-Ni cast steels in the HCl solution, Journal of Alloys and Compounds 598 (2010) 143-147.

[10] Cvijović Z., and Radenković, G., Microstructure and pitting corrosion resistance of annealed duplex stainless steel, Corrosion Science 48 (2006) 3887-3906.

[11] Hou, B. , Li, Y., Li, Y., Zhang, J., Effect of alloy elements on the anti-corrosion properties of low alloy steel, Bull. Mater. Sci. 23 (2000) 189-192.

[12] Zhang, L., Zhang, W., Jiang, Y., Deng, B., Sun, D., Li, J., Influence of annealing treatment on the corrosion resistance of lean duplex stainless steel 2101, Electrochimica Acta 54 (2009) 5387–5392.

[13] Choi, Y.-S., Kim, J.-G., Park, Y.-S., Park, J.-Y., Austenitzing treatment influence on the electrochemical corrosion behaviour of 0.3C-14Cr-3Mo martnesitic stainless steel, Materials Letters 61 (2007) 244-247

[14] Isfahany, A. N., Saghafian, H., Borhani, G., The effect of heat treatment on mechanical properties and corrosion behaviour of AISI420 martensitic stainless steel, Journal of Alloys and Compounds 509 (2011) 3931-3936

[15] Park, J.-Y., Park, Y.-S., The effects of heat-treatment parameters on corrosion resistance and phase transformation of 14Cr-3Mo martensitic stainless steel, Materials Science and Engineering A 449-451 (2007) 1131-1134

[16] Dyja, D., Stradomski, Z., Pirek, A., Microstructural and fracture analysis of aged cast duplex steel, Strength of Materials, Vol. 40, No. 1 (2008) 122-125

[17] Lucio-Garcia, M.A., Gonzalez-Rodrigueza, J.G., Casalesc, M., Martinezc, L., Chacon-Navaa, J.G., Neri-Floresa, M.A. and Martinez-Villafañea A., Effect of heat treatment on H_2S corrosion of a micro-alloyed C–Mn steel, Corrosion Science 51 (2009) 2380-2386

[18] Banaś, J., Lelek-Borkowska, U., Mazurkiewicz, B., Solarski, W., Effect of CO_2 and H_2S on the composition and stability of passive film on iron alloy in geothermal water, Electrochimica Acta 52 (2007) 5704-5714.

[19] Moreira, R.M., Franco, C.V., Joia, C.J.B.M., Giordana, S., Mattos, O.R., The effects of temperature and hydrodynamics on the CO_2 corrosion of 13Cr and 13Cr5Ni2Mo stainless steels in the presence of free acetic acid, Corrosion Science 46 (2004) 2987-3003.

[20] Seiersten, M., Material selection for separation, transportation and disposal of CO_2, Corrosion paper no. 01042 (2001).

[21] Choi, Y.-Y. and Nešić, S. Determining the corrosive potential of CO_2 transport pipline in high pCO2-water environments, Journal of Green House Gas Control 5 (2011) 788-797.

[22] Han, J., Zhang, J., Carey, J.W., Effect of bicarbonate on corrosion of carbon steel in CO_2-saturated brines, Journal of Green House Gas Control 5 (2011) 1680-1683.

[23] Pfennig, A., Kranzmann, A., 2012, Effect of CO_2 and pressure on the stability of steels with different amounts of Chromium in saline water, Corrosion Science 65 (2012) 441–452

[24] Pfennig, A., Linke, B., Kranzmann, A. Corrosion behavior of pipe steels ex-posed for 2 years to CO_2-saturated saline aquifer environment similar to the CCS-site Ketzin, Germany, Energy Procedia, Vol. 4 (2011) 5122-5129.

[25] Mu, L.J. Zhao, W.Z., Investigation on carbon dioxide corrosion behavior of HP13Cr110 stainless steel in simulated stratum water, Corrosion Science 52 (2010) 82-89.

[26] A. Pfennig, P. Zastrow, A. Kranzmann, Influence of heat treatment on the corrosion behaviour of stainless steels during CO_2-sequestration into saline aquifer, International Journal of Green House Gas Control 15 (2013) 213–224